Power production by a dynamic micro heat engine with integrated thermal switch

J. H. Cho, L. W. Weiss, C. D. Richards, D. F. Bahr, and R. F. Richards*

Washington State University, School of Mechanical and Materials Engineering
Pullman, WA 99164-2920, U.S.A.

Abstract

Power production by a dynamic micro heat engine with integrated thermal switch is been demonstrated. A micro engine operated from a constant heat source of 60°C is shown to produce ~350 μW. Employing an active thermal switch to control heat rejection from the micro engine enables engine power to be increased to ~1100 μW. Power consumption by the thermal switch is shown to be minimized by operating the cantilever switch at its resonant frequency. Thermal switch power requirements can be reduced to less than 10 μW, even for operations speeds of 100 Hz or more.

Keywords: Micro heat engine, Net power, Thermal switch, Micro power generator.

1 - INTRODUCTION

On the macro-scale, dynamic heat engines have achieved great success as power sources, much greater than either fuel cells or static heat engines. This success is in large part because dynamic heat engines are more fuel flexible than fuel cells and have achieved higher conversion efficiencies than static heat engines. This success has motivated a variety of designs for micro-scale dynamic heat engines. These include micro gas turbine (Brayton cycle) engines [1], micro rotary internal combustion (Otto cycle) engines [2] and micro steam turbine (Rankine cycle) engines [3].

Work in our lab has been directed toward the development of a MEMS power system based on a dynamic heat engine that is driven by an external heat source. Key to the success of this power system is the control of heat transfer into and out of the engine by a thermal switch. The thermal switch controls the timing and duration of the heat addition and heat rejection. Heat transfer into the engine from the thermal switch evaporates liquid working fluid in the engine. Mechanical power is then produced as the vapor-phase working fluid expands against a flexible membrane. Likewise, heat transfer out of the engine to the thermal switch condenses the vapor-phase working fluid back into liquid. This periodic change in volume of the working fluid drives the oscillation of a flexible membrane.
As shown in Fig. l, an individual engine consists of a cavity filled with a saturated, two-phase working fluid, bounded on the top and bottom by thin membranes. The bottom membrane acts as the evaporator. A capillary wick fabricated on the bottom membrane controls the layer of liquid-phase working fluid on the evaporator. The top membrane of the cavity is the part of the engine that does mechanical work.

In order to maximize the power output and mechanical efficiency of the engine, work in our group has focused on optimizing components for the engine, including the thermal switch responsible for controlling heat transfer into and out of the engine, the wicking evaporator fabricated on the bottom membrane of the engine that controls the flow and position of liquid-phase working fluid and the top membrane of the engine that functions as the expander.

Work on the thermal switch has been directed at the realization of a switch design in which an array of liquid-metal micro-droplets deposited on one silicon substrate makes and breaks contact with a second silicon substrate. The concept is illustrated in Fig. 2. Steady-state thermal measurements have shown in ref. 4 [4]. Dynamic thermal measurements have shown in ref. 5 [5].

Work on the wicking evaporator has focused on controlling the layer of liquid-phase working fluid on the bottom membrane evaporator. Both experimental and numerical work has shown that the primary factor controlling engine efficiency is the location and thickness of the liquid-phase working fluid. In particular, the design of the wicking

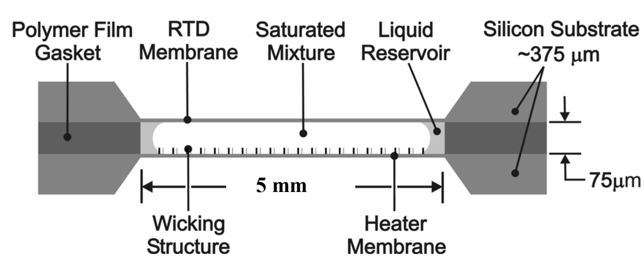

Figure 1 - Cross section of micro heat engine.

* Contact author: Tel. 509-335-8157, Fax: 509-335-4662, email: heatran@wsu.edu

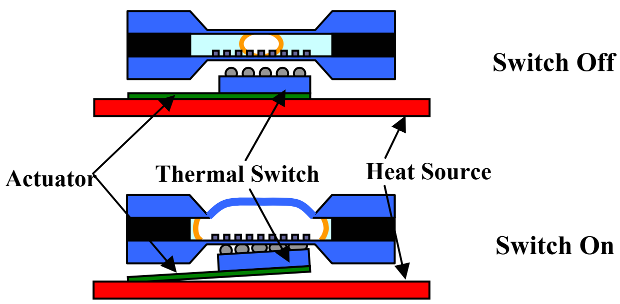

Figure 2 - Schematic of engine with cantilever switch.

structure that pumps and holds the thin film of liquid working fluid over the area of heat addition has been shown to significantly affect engine output and efficiency [6].

Work on the top membrane expander has identified the thermal mass of the top and bottom membranes and the compliance of the top membrane as secondary factors controlling engine efficiency. Reducing thermal mass and increasing compliance have both been shown to increase engine efficiency [7].

The purpose of this paper is to describe the operation of the dynamic micro heat engine with heat transfer to and from the engine controlled by the thermal switch. In particular, the major goals of the present work are: (1) to demonstrate engine operation from a continuous heat source by controlling heat addition using a thermal switch (2) to demonstrate increased engine cycle speed and performance by controlling and increasing heat rejection rates via a thermal switch and (3) to document the power budget required by a thermal switch to dynamically control heat transfer to and from the micro-engine.

2 - EXPERIMENT

The experimental work was conducted with the apparatus illustrated in Fig. 2. The experimental set-up included a single micro engine and thermal switch.

Each engine consisted of a cavity, defined by two silicon die, with square membranes bulk micromachined in them. The two die were clamped around a spacer and filled with a two-phase mixture of working fluid.

The top membranes, which functioned as expanders for the micro engines, were either five or eight millimeters on a side.

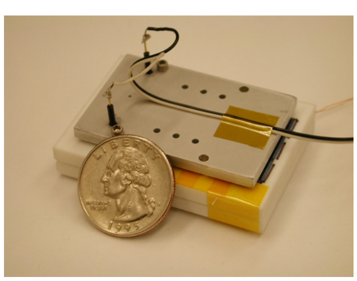

Figure 3 - Completed dynamic micro heat engine.

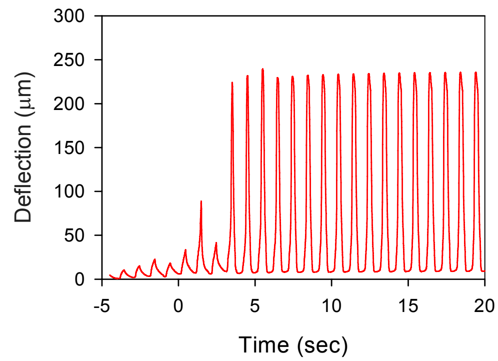

Figure 4 - Dynamic deflection of the top expander membrane of the engine at 1 Hz.

Both silicon and silicon nitride top membranes were fabricated. Silicon membranes were produced by boron doping the wafers and then wet etching to 2 microns. Silicon nitride membranes were produced by using an LPCVD process that left 300 nm silicon nitride atop the silicon wafers, then wet etching away the silicon.

The bottom membranes, which functioned as evaporators for the micro engines, were also five or eight millimeters on a side. Only two-micron thick silicon membranes were used as bottom membranes. Wicking structures were fabricated on the evaporator membranes by spinning a layer of SU-8 on them and then patterning photolithographically. Wicking structures were composed of SU-8 walls five microns thick that formed open-groove, rectangular cross-section capillaries with widths ranging from 10 to 90 microns and depths ranging from 10 to 90 microns.

Upon completion, the top and bottom die were clamped together, face to face, with semiconductor tape forming a gasket between them. Cavities with thicknesses of 75 and 150 microns were used. The cavities were filled with the working fluid 3M™ PF-5060DL.

The thermal switch controlling heat transfer to/from the micro engine took the form of a liquid-metal micro-droplet array (1600 thirty-micron droplets) deposited on a silicon die. The micro-droplet-array die was glued on the tip of a piezoelectric cantilever actuator. The cantilever thermal

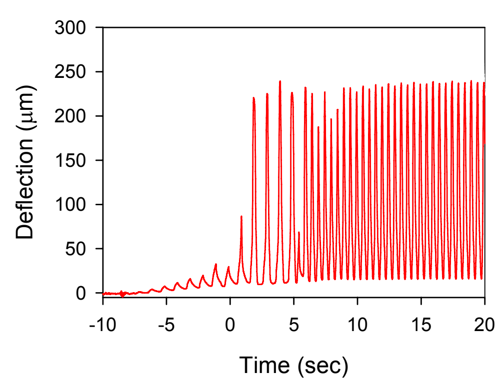

Figure 5 - Dynamic deflection of the top expander membrane of the engine at 2 Hz.

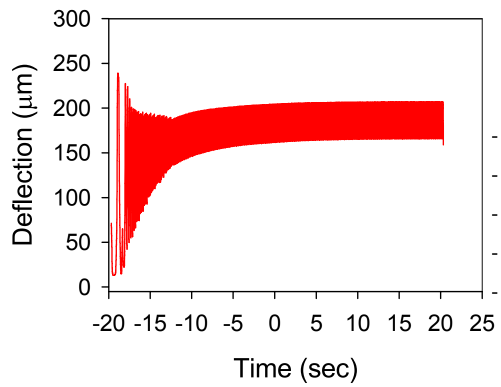

Figure 6 - Dynamic deflection of the top expander membrane of the engine at 16 Hz.

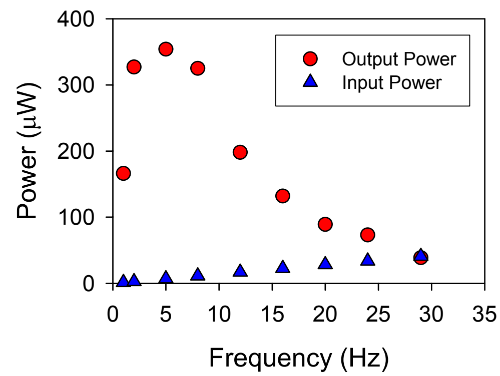

Figure 8 - Mechanical power out of the micro engine and mechanical power into the thermal switch as functions of micro engine cycle speed.

switch was then mounted immediately below the engine so that as the cantilever flexed the micro-droplet array would make contact with the bottom evaporator membrane. Figure 3 shows the fully assembled dynamic micro heat engine.

To run the engine, the cantilever thermal switch was heated to a constant temperature of 60 to 65°C. Heat transfer to the engine was then controlled by actuating the cantilever thermal switch to periodically make and break contact with the bottom evaporator membrane. The actuation frequency of the thermal switch thus controlled the cycle frequency of the engine.

The mechanical output of the micro-engine was determined using a laser vibrometer. The laser vibrometer was used to measure the deflection of the top membrane. Since the micro heat engine was operated far from resonance, the engine cavity pressure could be determined from the top membrane deflection using an experimentally determined pressure-deflection curve. Work done by the engine was then taken to be the boundary work done by the top expander membrane.

3 - RESULTS

The operation of the micro heat engine with heat addition from a constant temperature heat source at 60°C is illustrated in Figs. 4 through 8. In these experiments, heat rejection from the engine was by passive cooling to the surroundings at 20 °C.

Figures 4, 5 and 6 show the dynamic deflection of the top expander membrane of the engine versus time. In Fig. 4, with the engine cycling at 1 Hz, the maximum expander membrane deflection is ~240 microns. As the cycle speed is increased to 2 Hz in Fig. 5, the maximum and minimum expander membrane deflection increase slightly. As engine cycling speed is further increased, the maximum expander membrane deflection decreases slightly as the minimum deflection increases as seen in Fig. 6. In Fig. 6, maximum expander membrane deflection has decreased to ~210 microns while minimum ~160 microns. This decline in peak-to-peak membrane deflection with increasing engine cycle speed is plotted in Fig. 7. The mechanical power output of the micro engine versus engine cycle speed is shown in Fig. 8. The engine power is seen to rise to a maximum of ~350 μW at a cycle speed of 5 Hz and then decline. The primary reason for the decline in engine output is the rise in average engine temperature as engine cycle speed and thermal power into the engine increases.

Figure 8 also shows the power consumed by the cantilever thermal switch controlling heat addition to the micro engine. The thermal switch power is seen to rise linearly from ~1 μW

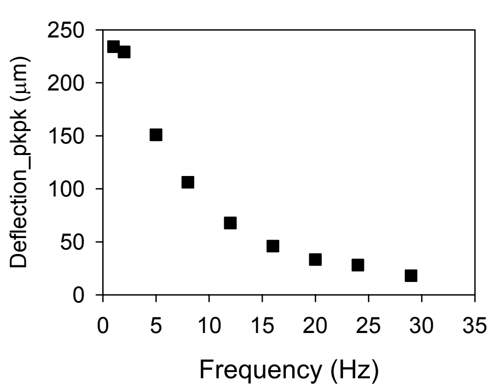

Figure 7 – Peak to peak deflection versus frequency.

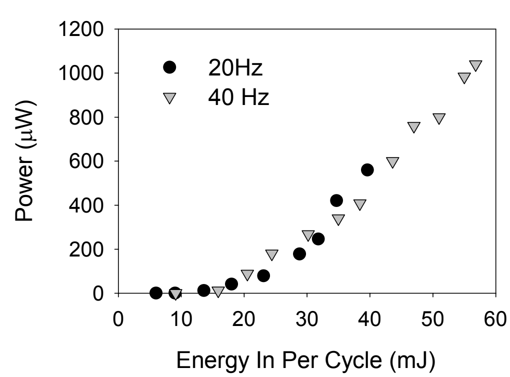

Figure 9 – Power output versus energy in per cycle.

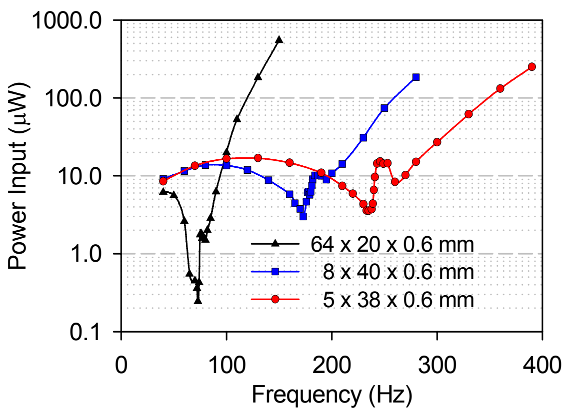

Figure 10 - Thermal switch power input versus frequency for three cantilever switches with 40 μm deflection.

at a cycle speed of 1Hz to ~40 μW at a cycle speed of 29 Hz At cycle speeds of 16 Hz and less, thermal switch power is a small fraction of engine output. However, above 24Hz, thermal switch power becomes a significant parasitic loss.

Figure 8 illustrates two serious concerns associated with higher cycle speeds: (1) declining engine power and (2) rising thermal switch power. These two concerns can be addressed by controlling heat rejection from the micro engine with an active thermal switch, and by running the cantilever thermal switch at its resonant frequency.

The first concern, declining engine power with higher cycle speeds, can be addressed by employing a thermal switch to actively cool the engine. Figure 9 shows power output versus energy in per cycle for a micro engine that is actively cooled by a thermal switch. Power data for cycle speeds of 20 and 40 Hz are plotted. The use of the thermal switch to actively control heat rejection from the engine is seen to dramatically increase the power output of the micro engine. Maximum power out of the micro engine increases to ~600 μW at a cycle speed of 20 Hz and to ~1100 μW at 40 Hz.

The second concern, the increasing power required to operate the thermal switch at higher cycle speeds, can be addressed by running the cantilever thermal switch at its resonant frequency. Figure 10 shows the power required to deflect three cantilever thermal switches 40 microns versus operating frequency. Thermal switch power is seen to reach minima of ~0.2, ~3 and ~4 μW for the respective resonant frequencies of ~70, ~170 and ~240 Hz of the three cantilever switches. This level of power consumption by the thermal switch represents a small parasitic power cost for an engine that produces 100's of μW of power.

4 - CONCLUSION

Power production by a dynamic micro heat engine with integrated thermal switch has been demonstrated. The thermal switch was used to control heat addition into the micro engine from a constant heat source at 60^{o}C. The maximum power out from a passively cooled micro engine was ~350 μW. Under this condition, the power required to run the thermal switch was ~7 μW. Decreases in engine power output were shown to be a consequence of rising average engine temperature. The use of an active thermal switch was shown to be an effective means to control heat rejection from the micro engine. Maximum power out from a actively cooled micro engine was ~1100 μW. Power consumption by the thermal switch was shown to be minimized by operating the cantilever switch at its resonant frequency. Thermal switch power requirements can be reduced to less than 10 μW, even for operations speeds of 100 Hz or more.

ACKNOWLEDGMENTS

The authors gratefully acknowledge the support provided by DARPA MTO's MicroPower Generation Program and the US Army SMDC under Contract No. DASG60–02–C0001and the NSF under grant CTS-0404370.

REFERENCES

[1] A.H. Epstein, "Millimeter-Scale, Micro-Electro-Mechanical Systems Gas Turbine Engines," *ASME J. of Eng. for Gas Turbines and Power*, Vol.126, pp. 205-226, 2004.
[2] K. Fu, A. J. Knobloch, F.C. Marinez, D.C. Walther, C. Fernandez-Pello, A.P. Pisano, D. Liepmann, "Design and Fabrication of a Silicon-Based MEMS Rotary Engine," *Proc. ASME IMECE* 2001, Paper No. MEMS-23925, New York 2001.
[3] L.G. Frechette, C. Lee, S. Arslan, Y-C. Liu, "Design of a Microfabricated Rankine Cycle Steam Turbine for Power Generation," *Proc. ASME IMECE 2003*, Paper No. MEMS , Wash. D.C. 2003.
[4] J. Cho, T. Wiser, C. Richards, D. Bahr and R. Richards, "Fabrication and Characterization of a Thermal Switch," *Sensors and Actuators: A. Physical*, In Press, 2006.
[5] J.H. Cho, C.D. Richards, J.Jiao, D.F. Bahr, R.F. Richards, "Design and Characterization of a MEMS Thermal Switch," *Solid-State Sensors, Actuators and Microsystems Workshop* 2006, Hilton Head Island, South Carolina, pp 272-275, 2006.
[6] S.A. Whalen, C. Richards, D. F. Bahr, and R. Richards, "Characterization and Modeling of a Microcapillary Driven of a Liquid-Vapor Phase-Change Membrane Actuator," *Sensors and Actuators: A. Physical*, In Press, 2006.
[7] L.W. Weiss, J. H. Cho, K.E. McNeil, D.F. Bahr, C.D. Richards, and R.F. Richards, "Characterization of a Dynamic Micro Heat Engine with Integrated Thermal Switch," Journal of *Micromechanics and Microengineering*, Vol. 16**,** pp S262-S269, 2006.